Available online at www.sciencedirect.com
SCIENCE DIRECT®
International Journal of Mass Spectrometry 238 (2004) 265–277
International Journal of Mass Spectrometry
www.elsevier.com/locate/ijms

Characterisation of poly(alkyl methacrylate)s by means of electrospray ionisation–tandem mass spectrometry (ESI–MS/MS)

Anthony T. Jackson[a,*], Susan E. Slade[b], James H. Scrivens[b]

[a] *ICI Measurement Science Group, Wilton Centre, Wilton, Redcar, Cleveland TS10 4RF, UK*
[b] *Department of Biological Sciences, University of Warwick, Coventry CV4 7AL, UK*

Received 6 September 2004; accepted 24 September 2004

Abstract

Electrospray ionisation–tandem mass spectrometry (ESI–MS/MS) has been employed for the characterisation of two poly(alkyl methacrylate) polymers, namely poly(methyl methacrylate) (PMMA) and poly(*n*-butyl methacrylate) (PBMA). Collision-induced dissociation (CID) experiments were performed in a quadrupole orthogonal time-of-flight (ToF) tandem mass spectrometer fitted with a nanospray source. Tandem mass spectra from singly, doubly and triply charged precursor ions (with alkali metals used for cationisation of the oligomers) are shown and the data are compared to those previously generated by means of matrix-assisted laser desorption/ionisation-collision-induced dissociation (MALDI-CID). These data indicate that cations with greater ionic radii may yield the most useful structural information as the mass-to-charge ratio of the precursor ion increases, whereas lithium or sodium ions are proposed to be ideal for obtaining spectra from lower molecular weight oligomers. Fragment ions at low mass-to-charge ratios dominate the spectra. Two series of peaks may be used to calculate the masses of the initiating and terminating end groups of the polymer. Ion peaks of greater mass-to-charge ratios form series that may be used to infer sequence information from the polymers.

Keywords: Poly(alkyl methacrylate); Poly(*n*-butyl methacrylate); Electrospray ionisation–tandem mass spectrometry; Collision-induced dissociation

1. Introduction

Mass spectrometry has increasingly become an important tool for the characterisation of synthetic polymers over the last decade [1–6], primarily due to the development of electrospray ionisation (ESI) [7,8] and especially matrix-assisted laser desorption/ionisation (MALDI) [9,10]. These ionisation techniques enable data to be obtained from synthetic polymers of relatively high molecular weights (up to approximately 1.5 MDa in advantageous cases [11]). Average molecular weight (for narrow polydispersity polymers, unless coupled with a separation technique such as gel-permeation chromatography (GPC)) and structural (including end group identification) information may be obtained.

Tandem mass spectrometry (MS/MS) has been employed for the generation of further structural information from synthetic polymers. Initial reports of MS/MS studies used magnetic sector instrumentation [12–14], with more recent reports from a variety of instruments, including tandem hydrid sector-quadrupole [15–18], tandem hydrid sector-time-of-flight (ToF) [19–28], tandem quadrupole-orthogonal ToF [29], ion trap [30–32] and Fourier-transform ion cyclotron resonance (FTICR) mass spectrometers [33]. Most reports have used collision-induced dissociation (CID) to induce fragmentation of the selected precursor ions. Electron-capture dissociation (ECD) has also shown to be useful for activation of certain types of polymers [33], but is limited to use in FTICR instruments. Furthermore, the pseudo-MS/MS experiment called post-source decay (PSD) has been employed in MALDI-ToF instruments for structural characterisation of synthetic polymers [20,34]. This latter technique, however, suffers from a low selectivity of the precursor ion mass-to-

* Corresponding author. Tel.: +44 1642 435720; fax: +44 1642 435777.
E-mail address: tony_jackson@ici.com (A.T. Jackson).

1387-3806/$ – see front matter © 2004 Elsevier B.V. All rights reserved.
doi:10.1016/j.ijms.2004.09.026

charge ratio (m/z) and a lack of control of ion activation conditions.

The combined mass of the end groups of a polymer may be calculated from mass spectrometric data, but the masses of the individual (i.e. both initiating and terminating) end groups may often be generated from MS/MS spectra [19]. Sequence information from synthetic polymers and copolymers may also be generated by means of MS/MS. Sequencing of a block methyl methacrylate/*n*-butyl methacrylate (MMA/BMA) copolymer [23] and a tri-block ethylene oxide/propylene oxide/ethylene oxide (EO/PO/EO) copolymer [33] has been described.

Two poly(alkyl methacrylate) polymers have been characterised by means of ESI–MS/MS, in a tandem quadrupole-orthogonal ToF instrument, in this study. Spectra have been obtained from singly, doubly and triply charged precursor ions and the results are compared to those obtained from the same polymers (from singly charged precursors) by means of MALDI-CID in a tandem hydrid sector-ToF mass spectrometer. The effect of varying the alkali metal cation, on the resulting tandem mass spectra, is compared for ESI–MS/MS experiments.

2. Experimental

2.1. Mass spectrometry

ESI–MS/MS experiments were performed in a Q-ToF Global (Waters MS Technologies, Manchester, UK) tandem quadrupole-orthogonal ToF instrument, fitted with a nanospray source. The instrument was calibrated from m/z 50 to 4000 with sodium iodide, such that the mass accuracy for these experiments was expected to be within approximately 0.025%. The source temperature was 80 °C and the capillary voltage set at 1.5 kV. Precursor ions were selected by the quadrupole such that the whole isotope cluster was passed to the collision cell. The collision energy (E_{coll}) was varied between 60 and 120 eV in these experiments (the values for each experiment are detailed in Figure legends) and the collision gas was argon.

2.2. Sample preparation

The PMMA A (**1**) and PBMA A (**2**) standards were obtained from Polymer Laboratories (Church Stretton, UK) and Viscotek (Basingstoke, UK), respectively, and used without further purification. The most probable mass or peak average molecular weight (M_p) and polydispersity values of these polymers, which are estimated by the manufacturer using GPC, are 2400 and 1.08 for PMMA A and 3670 and 1.08 for PBMA A. Lithium acetate, sodium acetate, potassium acetate, rubidium acetate and caesium acetate were from Sigma (Steinheim, Germany). HPLC grade methanol was from Aldrich (Gillingham, UK).

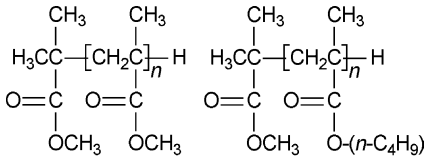

All solutions were prepared at a concentration of approximately 1 mg mL^{-1} in methanol. Solutions of the analyte and alkali metal salt were mixed in a ratio of 100:1 (v/v) prior to addition of 20 μL to the nanospray needle.

3. Results and discussion

3.1. ESI–MS/MS of poly(methyl methacrylate)

The electrospray mass spectra of PMMA A (data not shown) are dominated by doubly charged ions, with a lower level of singly charged ions also present. These ions are all of the type $[\mathbf{1} + Cat]^+$ and $[\mathbf{1} + 2Cat]^{2+}$, where Cat is an alkali metal cation from the salts employed to aid cationisation of the oligomers of PMMA A (**1**). It has been shown previously (for oligomeric ions generated by MALDI) that the carbonyl oxygens, of the ester side-chains in PMMA, have an affinity for alkali metal cations [35]. It was proposed that it is these carbonyl oxygens, from side-chains near both of the chain ends of the oligomer that interact with alkali metal cations and that the ions have a U-shape. It is presumed that the singly charged ions generated in ESI–MS experiments are similar in nature, but ion mobility experiments would be required to investigate further.

Initially, singly charged precursor ions (i.e. $[\mathbf{1} + Cat]^+$) were chosen for study by means of ESI–MS/MS, in order that the data could be compared to that obtained previously by means of MALDI-CID [20]. The ESI–MS/MS spectra from the 18-mer of PMMA A ($[\mathbf{1} + Cat]^+$) are shown in Fig. 1, where Cat is lithium, sodium, potassium, rubidium or caesium. These spectra are dominated by fragment ions of low m/z (below m/z 600). The low m/z regions of these spectra are also shown expanded in Fig. 1. This region of the spectra is annotated with proposed assignments. The bare cation (i.e. Rb^+ and Cs^+) is the most intense ion peak in the spectrum from $[\mathbf{1} + Rb]^+$ and $[\mathbf{1} + Cs]^+$ precursor ions (spectra were acquired to a lower limit of m/z 50, so other bare alkali metal cations were not detected in these experiments). It was previously shown [20] that the peak from the bare cation is more intense in MALDI-CID spectra from alkali metal cations with a greater ionic radius. This is also indicated by the ESI–MS/MS data shown in Fig. 1 (albeit only from comparison of spectra from $[\mathbf{1} + Rb]^+$ and $[\mathbf{1} + Cs]^+$ precursor ions), where the Cs^+ ion dominates the spectrum from the $[\mathbf{1} + Cs]^+$ precursor ion but the Rb^+ ion is of similar intensity to the other fragment ions in the lower m/z region of the spectrum from the $[\mathbf{1} + Rb]^+$ precursor ion.

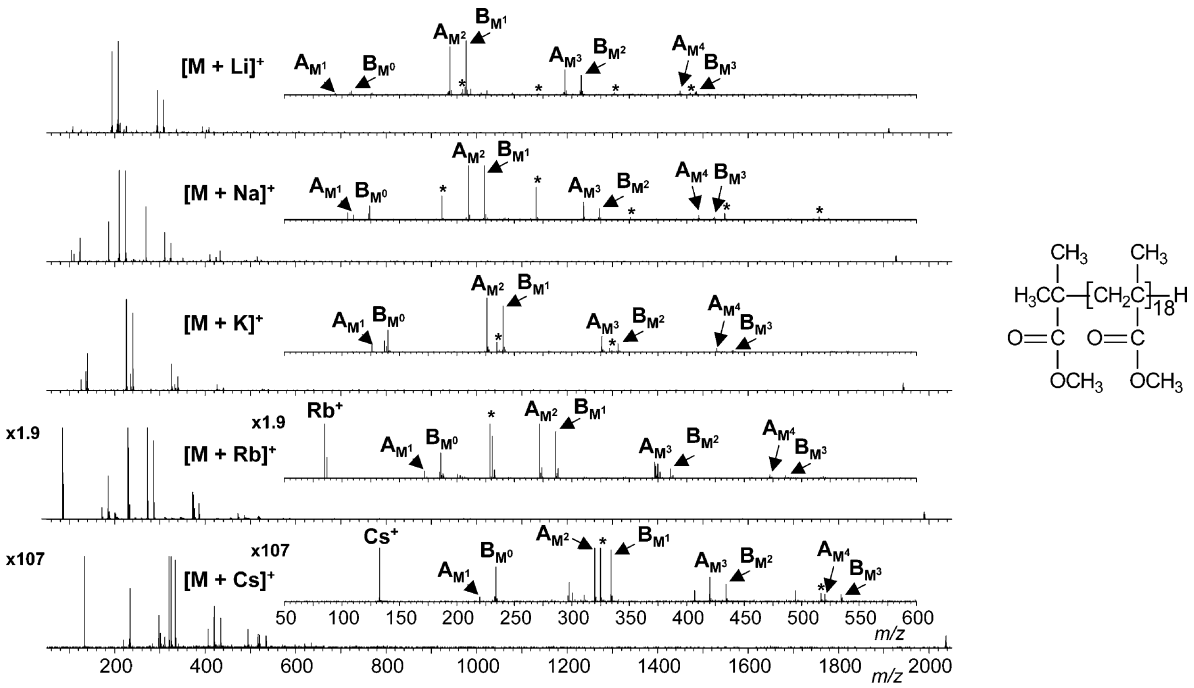

Fig. 1. ESI–MS/MS spectra (E_{coll} = 105 eV) from the 18-mer of PMMA A ([**1** + Cat]$^+$), where Cat is lithium, sodium, potassium, rubidium or caesium (*peaks from alkali metal (Cat) acetate (Ac) clusters of the type [Cat$_x$Ac$_{x-1}$]$^+$). Annotated expansions of the *m*/*z* 50–600 region are also shown (see text for explanation of peak annotation).

Two series of fragment ion peaks are seen in the low *m*/*z* regions of all the spectra shown in Fig. 1 that are separated by *m*/*z* 100, which is equivalent to the repeat unit mass of PMMA oligomers. These peaks have been annotated in the expansions of the spectra in Fig. 1. This nomenclature for this annotation is similar to that described previously from MALDI-CID results [24]. The **A** series of fragment ion peaks are proposed to arise from fragmentation with charge retention (i.e. the alkali metal cation) at the terminating (ω) end of the oligomer and the **B** series from the initiating (α) end. This propounded fragmentation of PMMA is described by Scheme 1. The fragmentation nomenclature differs slightly from that shown previously in that the subscript describes the monomer (**M** represents methyl methacrylate, MMA) and the number of (whole or partial) units of this monomer in the fragment ion (i.e. $\mathbf{A_{M2}}$ represents a fragment ion from the terminating end of the oligomer that contains two (one partial) unit of MMA). This nomenclature has been developed as it will describe the fragmentation of both of homopolymers and copolymers (tandem mass spectrometry has previously been used to sequence an acrylic copolymer [23]).

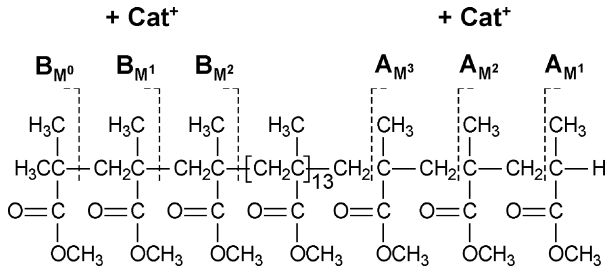

Scheme 1. Proposed fragmentation scheme for the **A** and **B** series of PMMA A.

Four peaks from each of the **A** and **B** series are seen in the spectra for each cation (see expansions of all five spectra in Fig. 1). The masses of the end groups may be calculated from the mass-to-charge ratios of these fragment ions by using the following equations [20]:

$$m/z(\mathbf{A}_{\mathbf{M}n}) = M(\omega) + M(n\mathbf{M}) - M(\mathrm{CH_2}) + M(\mathrm{Cat}), \qquad \mathbf{A}\ \text{Series} \tag{1}$$

$$m/z(\mathbf{B}_{\mathbf{M}n}) = M(\alpha) + M(n\mathbf{M}) + M(\mathrm{Cat}), \qquad \mathbf{B}\ \text{Series} \tag{2}$$

where $m/z(\mathbf{A}_{\mathbf{M}n})$ and $m/z(\mathbf{B}_{\mathbf{M}n})$ are the mass-to-charge ratios of a peak from the **A** and **B** series, respectively, that contain *n* monomer units of MMA (**M**), *M*(ω) and *M*(α) are the masses of the ω and α end groups, respectively, *M*(*n***M**) is the mass of *n* units of MMA and *M*(Cat) is the mass of the cation. The masses (*M*(α) and *M*(ω), respectively) of these end groups for PMMA A are 101.06 Da for the α (initiating) and 1.01 Da for the ω (terminating) end groups. The calculated *m*/*z* (i.e. $m/z(\mathbf{A_{M2}})$) for the sodiated fragment ion from the terminating end of the chain, for example, that contains two (one partial) units of MMA is 210.09 compared to the experimental value of *m*/*z* 210.14 (within the expected error for the calibration employed in these experiments). It should be noted that much better mass accuracy could be obtained with

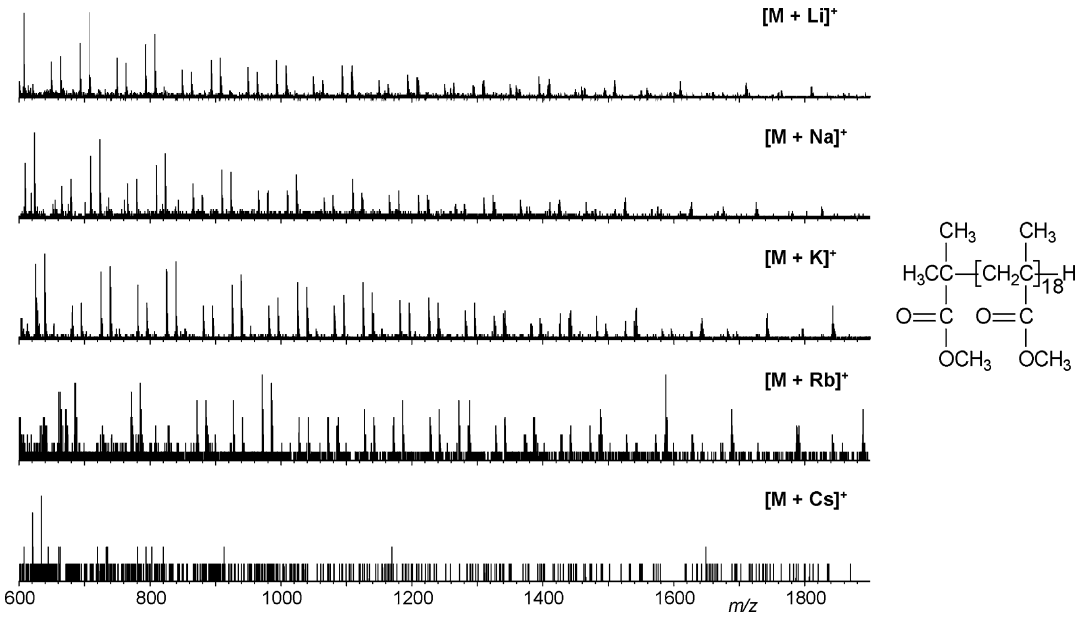

Fig. 2. Expansions (*m*/*z* 600–1900) of the ESI–MS/MS spectra from the 18-mer of PMMA A ([**1** + Cat]$^+$), where Cat is lithium, sodium, potassium, rubidium or caesium.

this instrumentation if a Lockspray^{TM} source is employed [29].

The fragment ions of the **A** and **B** series are radical cations for which mechanisms of formation have been previously proposed [20,35]. Another series of fragment ion peaks of lower intensity is also present in all five spectra (not annotated in Fig. 1), at the same mass-to-charge ratios as those previously proposed to arise from rearrangement reactions (to form even electron fragment ions). These ion peaks were previously annotated as the **G** series and were observed from low mass-to-charge ratios up to those much higher than that of the **A** and **B** series. The calculated mass-to-charge ratios of ions from the **G** series may be calculated using the equation below [24]:

$$m/z(\mathbf{G}_{\mathbf{M}n}) = M(n\mathbf{M}) + M(\mathrm{Cat}), \qquad \mathbf{G}\ \text{Series} \tag{3}$$

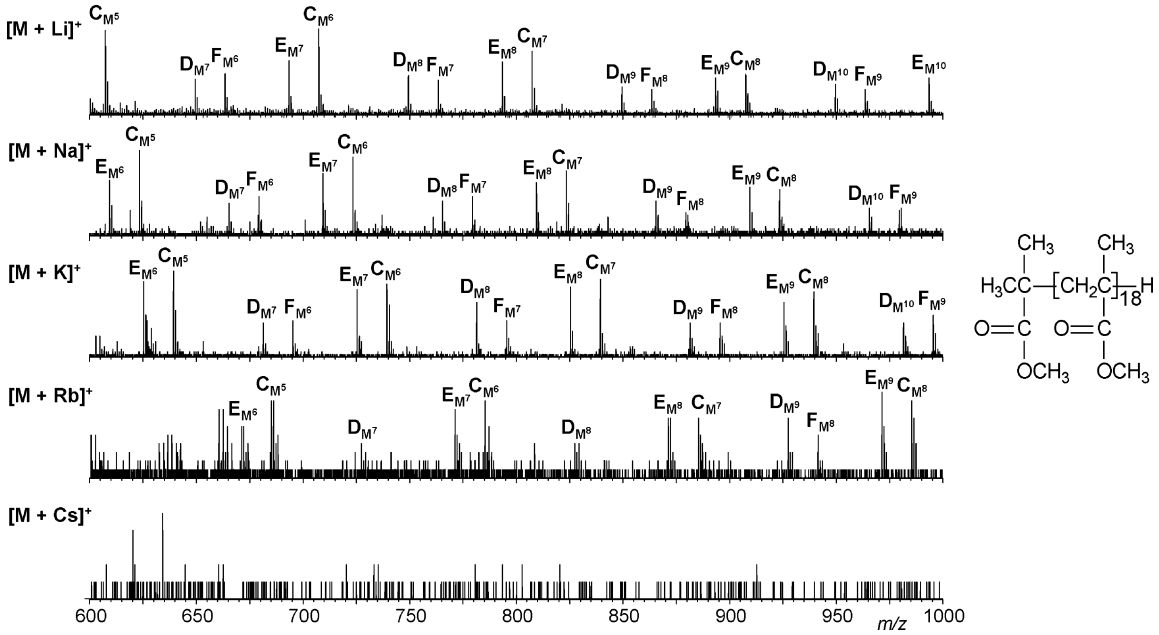

Fig. 3. Annotated expansions (*m*/*z* 600–1000) of the ESI–MS/MS spectra from the 18-mer of PMMA A ([**1** + Cat]$^+$), where Cat is lithium, sodium, potassium, rubidium or caesium (see text for explanation of peak annotation).

where $m/z(\mathbf{G}_{\mathbf{M}n})$ is the mass-to-charge ratio of a peak from the **G** series and $M(n\mathbf{M})$ and $M(\mathrm{Cat})$ are as described above for Eqs. (1) and (2).

Expansions of the higher mass-to-charge ratio regions (m/z 600–1900) of the spectra from $[\mathbf{1}+\mathrm{Cat}]^+$ singly charged precursor ions of PMMA (full spectra shown in Fig. 1) are displayed in Fig. 2. Four series of fragment ion peaks can be discerned in all spectra (albeit at relatively low signal-to-noise ratios in the spectrum from the $[\mathbf{1}+\mathrm{Rb}]^+$ precursor ion) except for that from the $[\mathbf{1}+\mathrm{Cs}]^+$ precursor ion, for which each peak in the series are separated by m/z 100, equivalent to the mass of the repeat unit of the PMMA.

A further expansion (m/z 600–1000) of the spectra is shown in Fig. 3, in which fragment ion peaks are annotated corresponding to the proposed series structures displayed in Scheme 2. Each of these series is proposed to arise from fragment ions that contain an intact end group from either the initiating (**C** and **F** series) or terminating (**D** and **E** series) moieties. The annotation of these peaks is again a slight modification of that described previously from MALDI-CID data of PMMA polymers [20], in that the number of repeat units of the polymer is added as a subscript (e.g. $\mathbf{C}_{\mathbf{M}7}$ contains seven units of MMA). It was previously propounded [24] and shown [23] that the ions from these four series could be used to differentiate between block and random copolymers. This slight change in proposed annotation is designed to cover the fragmentation of copolymers as well as homopolymers and is analogous to that used for the fragmentation of peptides (with the inclusion of the monomer descriptor). Mechanisms for formation of ions from these four series of ion peaks were previously proposed, from MALDI-CID data, which involved neutral losses from the precursor ions [24].

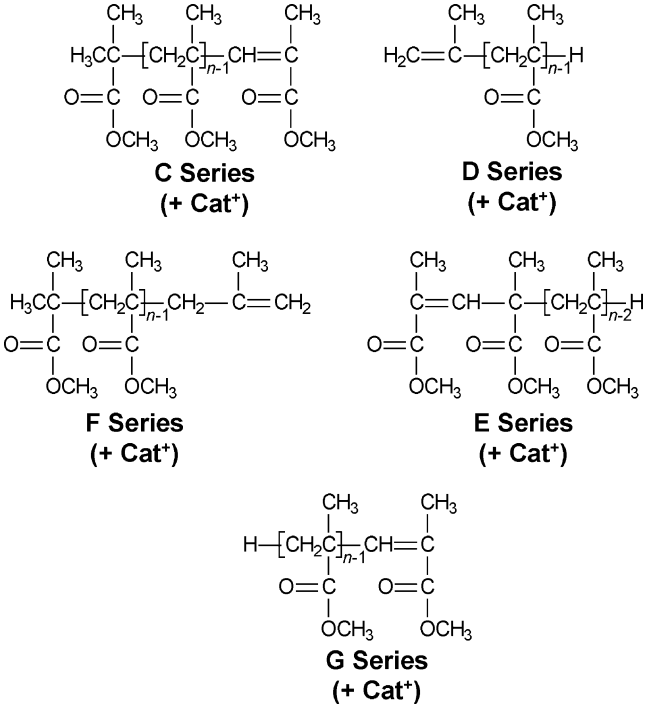

Scheme 2. Proposed structures for the **C**, **D**, **E**, **F** and **G** series of PMMA A.

The mass-to-charge ratios of these four series may be calculated from the following equations [24]:

$$m/z(\mathbf{C}_{\mathbf{M}n}) = M(\alpha) + M(n\mathbf{M}) - M(\mathrm{H}) + M(\mathrm{Cat}), \quad \mathbf{C}\ \text{Series} \tag{4}$$

$$m/z(\mathbf{D}_{\mathbf{M}n}) = M(\omega) + M(n\mathbf{M}) - M(\mathrm{C_2H_3O_2}) + M(\mathrm{Cat}), \quad \mathbf{D}\ \text{Series} \tag{5}$$

$$m/z(\mathbf{E}_{\mathbf{M}n}) = M(\omega) + M(n\mathbf{M}) - M(\mathrm{CH_3}) + M(\mathrm{Cat}), \quad \mathbf{E}\ \text{Series} \tag{6}$$

$$m/z(\mathbf{F}_{\mathbf{M}n}) = M(\alpha) + M(n\mathbf{M}) - M(\mathrm{CHO_2}) + M(\mathrm{Cat}), \quad \mathbf{F}\ \text{Series} \tag{7}$$

where $m/z(\mathbf{C}_{\mathbf{M}n})$, $m/z(\mathbf{D}_{\mathbf{M}n})$, $m/z(\mathbf{E}_{\mathbf{M}n})$ and $m/z(\mathbf{F}_{\mathbf{M}n})$ are the mass-to-charge ratios of a peak from the **C**, **D**, **E** and **F** series, respectively, and $M(\alpha)$, $M(\omega)$, $M(n\mathbf{M})$ and $M(\mathrm{Cat})$ are as described above for Eqs. (1) and (2).

These data from ESI–MS/MS of singly charged precursor ions are very similar to that obtained previously by means of MALDI-CID in a tandem hydrid sector-ToF mass spectrometer [19,20]. Fragment ion peaks (predominantly radical cations) in the low m/z region of the spectra are dominant, with peaks at lower intensity at higher mass-to-charge ratios (that are proposed to be formed by neutral losses from the precursor ions). These similarities in the spectra obtained under quite different conditions for the CID experiment (and using another ionisation technique), with ESI–MS/MS data obtained with low energy CID and MALDI-CID with high energy CID (800 eV and xenon as the collision gas), are dissimilar to that found for peptides. Significant differences (e.g. side-chain cleavages) are seen between the low energy CID and high energy CID of peptides. Furthermore, significant differences are often observed in low energy CID spectra from singly charged and doubly charged (protonated) precursor ion of peptides, often as a result of differences in charge location. A comparison between doubly and singly charged ions from PMMA oligomers was enabled by generating data from $[\mathbf{1}+2\mathrm{Cat}]^{2+}$ precursors to compare with the data from $[\mathbf{1}+\mathrm{Cat}]^+$ ions described above.

The ESI–MS/MS spectra from the doubly charged precursors of the 18-mer of PMMA A ($[\mathbf{1}+2\mathrm{Cat}]^{2+}$) are shown in Fig. 4, where Cat is lithium, sodium, potassium, rubidium or caesium. The spectra (as from the singly charged precursor, $[\mathbf{1}+\mathrm{Cat}]^+$, of the same oligomer that is shown in Fig. 1) from these precursors are again dominated by singly charged fragment ions in the low m/z region. This area (m/z 50–600) of the spectra is expanded and peaks are annotated in Fig. 4. The annotation is as described from singly charged precursors

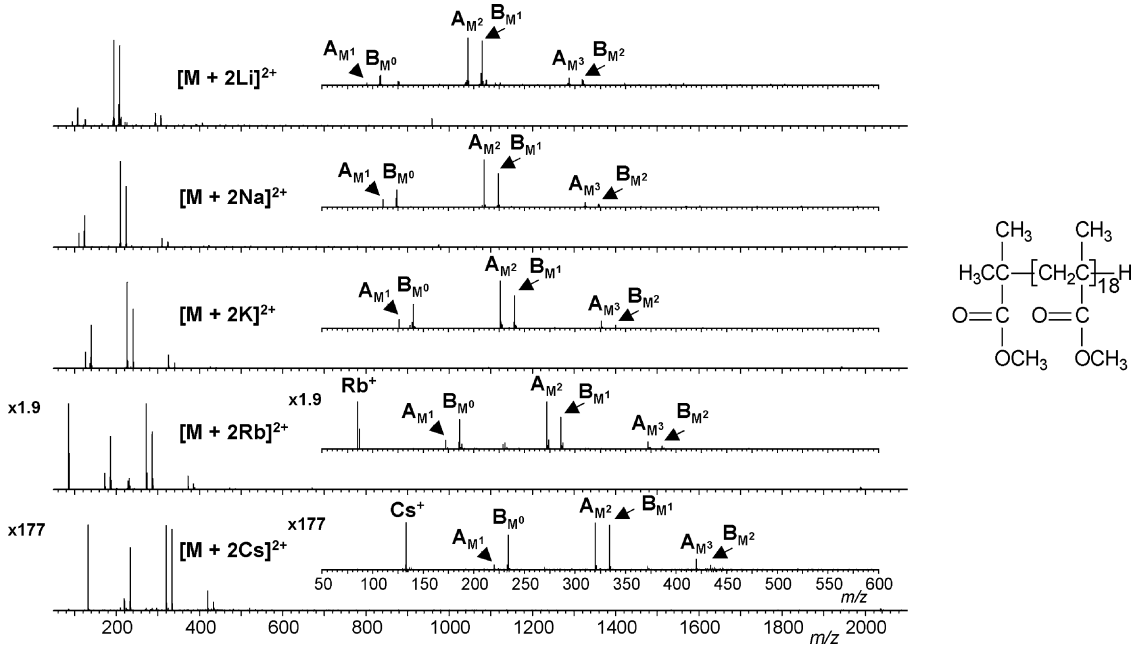

Fig. 4. ESI–MS/MS spectra (E_{coll} = 60 eV) from the 18-mer of PMMA A ([**1** + 2Cat]$^{2+}$), where Cat is lithium, sodium, potassium, rubidium or caesium. Annotated expansions of the *m/z* 50–600 region are also shown (see text for explanation of peak annotation).

(vide supra) and the proposed fragmentation scheme shown above (Scheme 1). The bare cations again are dominant from [**1** + Rb]$^+$ and [**1** + Cs]$^+$ precursor ions (spectra were again acquired to a lower limit of *m/z* 50, so other bare alkali metal cations were not detected), with the Cs^+ ion peak again relatively more intense (over two orders of magnitude more intense than that of the other low *m/z* fragments).

The distributions of fragment ion peaks from the **A** and **B** series, which may be used to calculate the masses of the end groups of the polymer as described above in Eqs. (1) and (2), are similar in all five spectra in Fig. 4 and are also comparable to those from singly charged precursor ions (Fig. 1).

The higher *m/z* region of these spectra is displayed in Fig. 5, with residual precursor ion peaks and peaks resulting from loss of one cation (e.g. [M + Na]$^+$) annotated. Four series of fragment ions, again all separated by *m/z* 100, may clearly be discerned in this region of all the spectra except that from the [**1** + 2Cs]$^{2+}$ precursor ion. These singly

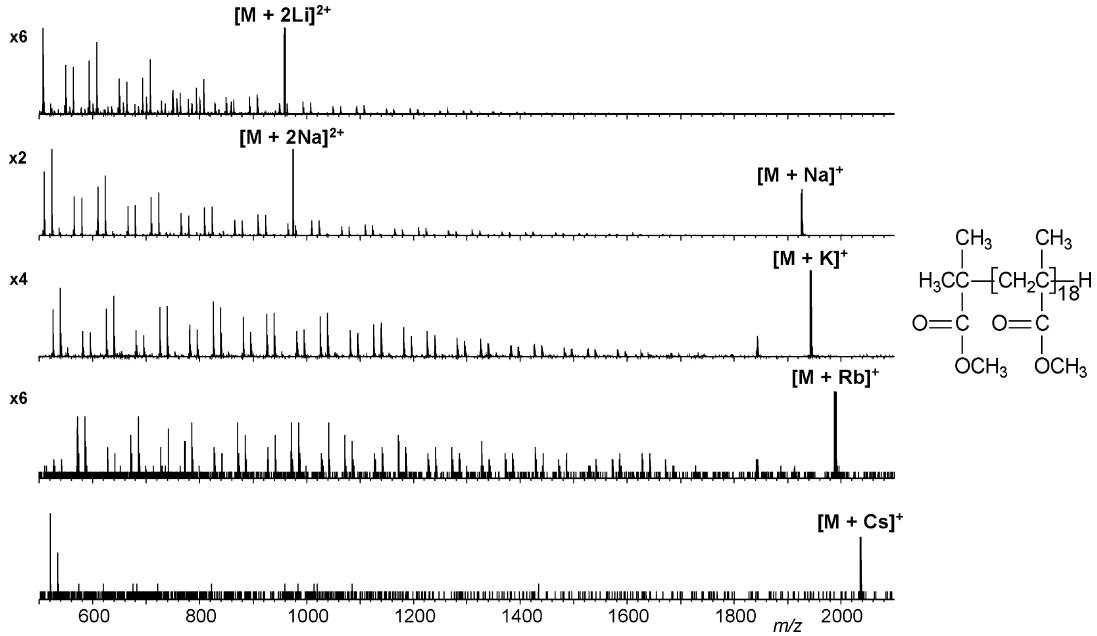

Fig. 5. Expansions (*m/z* 500–2100) of the ESI–MS/MS spectra from the 18-mer of PMMA A ([**1** + 2Cat]$^{2+}$), where Cat is lithium, sodium, potassium, rubidium or caesium.

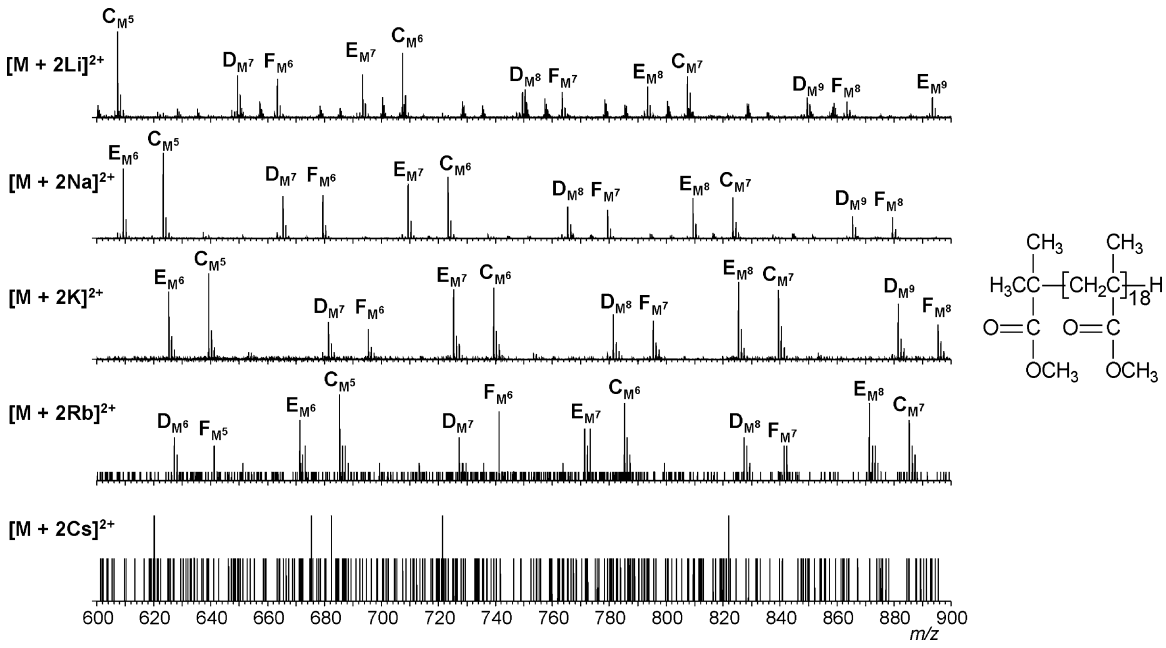

Fig. 6. Annotated expansions (*m*/*z* 600–900) of the ESI–MS/MS spectra from the 18-mer of PMMA A ([**1** + 2Cat]$^{2+}$), where Cat is lithium, sodium, potassium, rubidium or caesium (see text for explanation of peak annotation).

charged fragment ion peaks have a relatively high signal-to-noise ratio, except in the spectrum from the [**1** + 2Rb]$^{2+}$ precursor. Furthermore, doubly charged fragment ion peaks are observed at significant intensities in the spectrum from the lithiated precursor and at significantly lower intensities in that from the [**1** + 2Na]$^{2+}$ precursor ion. The peaks in these series are separated by *m*/*z* 50 and the difference between isotope peaks is *m*/*z* 0.5, indicating that these moieties are fragment ions relating to cleavage of the polymer chain.

A further expansion (*m*/*z* 600–900) of this region of the spectra is shown in Fig. 6. Singly charged fragment ion peaks from the **C**, **D**, **E** and **F** series are annotated as for the spectra from the singly charged precursor ions (Fig. 3). These regions of the spectra are very similar, in fact, from both singly and doubly charged precursors, except for the presence of some doubly charged fragment ions (especially in the spectrum from [**1** + 2Li]$^{2+}$) which are not annotated. The changes to lower signal-to-noise ratio for fragments from precursors containing higher radii cations (especially noticeable when comparing spectra from potassiated to caesiated precursors) are mirrored in both sets of spectra.

The doubly charged fragment ion peaks are also proposed to be from the fragments of the **C**, **D**, **E** and **F** series, where both of the cations are retained. These fragment ions are more abundant from moieties with greater numbers of monomer units (i.e. where *n* is higher for the structures in Scheme 2).

These data indicate that both singly and doubly charged precursor ions may be selected in the ESI–MS/MS experiment to generate, essentially, very similar results. The **A** and **B** series of fragment ions may be used to calculate the masses of the end groups of the polymer from both singly and doubly charged precursors. In addition, sequence specific ion peaks (the **C**, **D**, **E** and **F** series) are also observed in both sets of spectra, albeit with some doubly charged fragments from these series becoming more prevalent from precursors with lower radii cations.

3.2. ESI–MS/MS of poly(n-butyl methacrylate)

Doubly ([**2** + 2Cat]$^{2+}$) and triply ([**2** + 3Cat]$^{3+}$) charged ions are the dominant species, from intact oligomers, giving rise to peaks in the electrospray mass spectra from PBMA A (data not shown). Doubly charged precursor ions were initially selected for ESI–MS/MS experiments and the data compared to that obtained previously from singly charged precursor ions of the same polymer by means of MALDI-CID [24]. The ESI–MS/MS spectra from the 28-mer of PBMA A ([**2** + 2Cat]$^{2+}$) are shown in Fig. 7. Annotated expansions of the low *m*/*z* regions (*m*/*z* 50–600) of these product ion spectra are also displayed. Fragment ion peaks in this area of the spectra are again dominant, as noted from MALDI-CID experiments from this polymer [24] and observed from ESI–MS/MS of PMMA A (vide supra).

Peaks from bare cations (Rb^+ and Cs^+) are seen in the spectra from the respective precursors with these cations, with the peak from the caesium ion dominating this fragment ion spectrum (as seen for PMMA A in Figs. 1 and 4). The Rb^+ cation peak is again seen at similar intensity to many of the other fragment ion peaks in the low *m*/*z* region of the spectrum from the [**2** + 2Rb]$^{2+}$ precursor, as was observed from ESI–MS/MS spectra from PMMA A.

Two series of fragment ion peaks are seen in the low *m*/*z* regions of all the spectra shown in Fig. 7 that are separated by

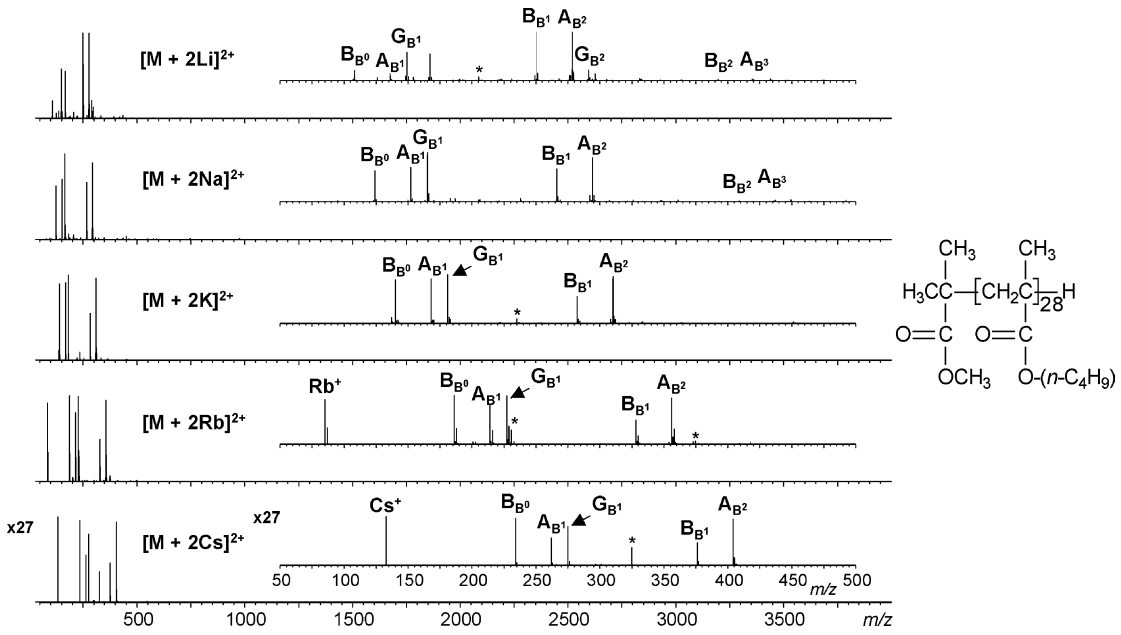

Fig. 7. ESI–MS/MS spectra (E_{coll} = 120 eV) from the 28-mer of PBMA A ([**2** + 2Cat]$^{2+}$), where Cat is lithium, sodium, potassium, rubidium or caesium (* peaks from alkali metal (Cat) acetate (Ac) clusters of the type [Cat_xAc_{x-1}]$^+$). Annotated expansions of the *m*/*z* 50–500 region are also shown (see text for explanation of peak annotation).

m/*z* 142, which is equivalent to the repeat unit mass of PBMA oligomers (annotated as the **A** and **B** series in the expansion in Fig. 7, with three peaks from each series observed in every one of the spectra). The nomenclature for this annotation is again slightly modified from that described previously from MALDI-CID results [24], where the **A** series of fragment ion peaks are proposed to arise from fragmentation with charge retention (i.e. the alkali metal cation) at the terminating (ω) end of the oligomer and the **B** series from the initiating (α) end. A propounded fragmentation map for the **A** and **B** series in PBMA A is displayed in Scheme 3. The subscript again describes the monomer (**B** represents *n*-butyl methacrylate (BMA)) and the number of (whole or partial) units of this monomer in the fragment ion (i.e. $\mathbf{A_{B2}}$ represents a fragment ion from the terminating end of the oligomer that contains two (one partial) unit of BMA). The structures of the fragment ions of the **A** and **B** series (radical cations) are proposed to be analogous to that from PMMA A (vide supra) [20,24].

Equations are shown below to describe how the masses of the end groups may be calculated from the mass-to-charge ratios of the fragment ion peaks of the **A** and **B** series:

$$m/z(\mathbf{A}_{\mathbf{B}n}) = M(\omega) + M(n\mathbf{B}) - M(CH_2) + M(\text{Cat}), \qquad \mathbf{A}\ \text{Series} \tag{8}$$

$$m/z(\mathbf{B}_{\mathbf{B}n}) = M(\alpha) + M(n\mathbf{B}) + M(\text{Cat}), \qquad \mathbf{B}\ \text{Series} \tag{9}$$

where $m/z(\mathbf{A}_{\mathbf{B}n})$ and $m/z(\mathbf{B}_{\mathbf{B}n})$ are the mass-to-charge ratios of a peak from the **A** and **B** series, respectively, that contain *n* monomer units of BMA (**B**), *M*(ω) and *M*(α) are the masses of the ω and α end groups, respectively, *M*(*n***B**) is the mass of *n* units of BMA and *M*(Cat) is the mass of the cation. The masses [*M*(α) and *M*(ω), respectively] of these end groups for PBMA A are 101.06 Da for the α (initiating) and 1.01 Da for the ω (terminating) end groups (i.e. the same as for PMMA A). The calculated *m*/*z* (i.e. $m/z(\mathbf{A_{B2}})$) for the sodiated fragment ion from the terminating end of the chain, for example, that contains two (one partial) units of BMA is 294.18 compared to the experimental value of *m*/*z* 294.23 (within the expected error for the calibration employed in these experiments).

Ion peaks from the **G** series are annotated in the expansions of the spectra displayed in Fig. 7. The structures of these moieties are proposed to be analogous to that shown above for PMMA A and as described previously from MALDI-CID results of singly charged precursors from PBMA A [24]. The mass-to-charge ratios of these ion peaks may be calculated by means of the equation shown below:

$$m/z(\mathbf{G}_{\mathbf{B}n}) = M(n\mathbf{B}) + M(\text{Cat}), \qquad \mathbf{G}\ \text{Series} \tag{10}$$

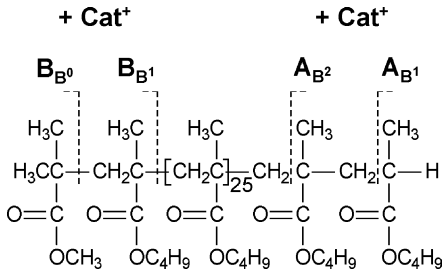

Scheme 3. Proposed fragmentation scheme for the **A** and **B** series of PBMA A.

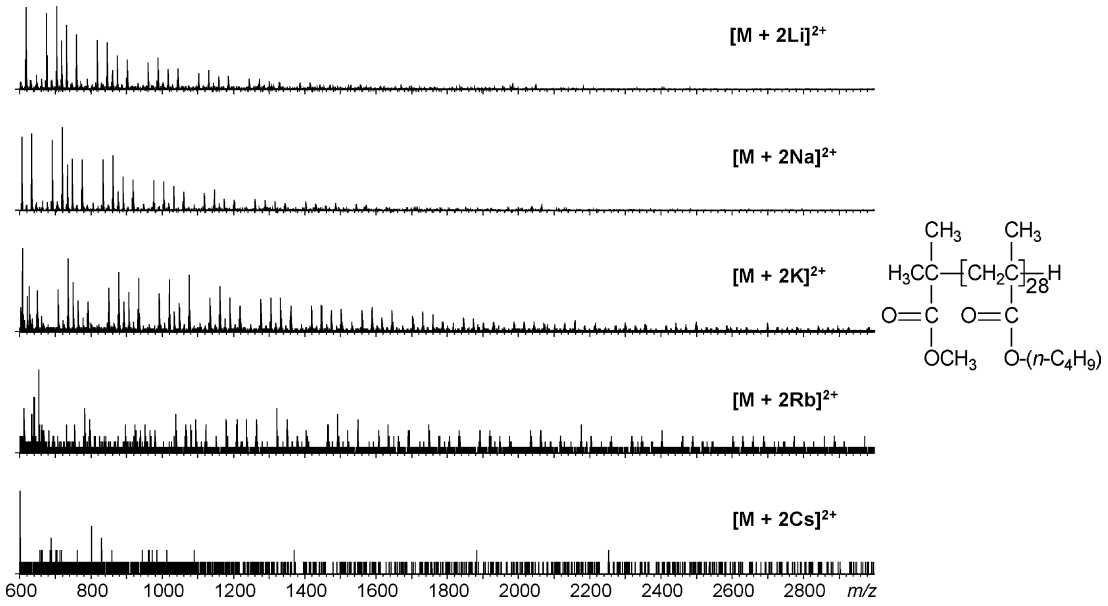

Fig. 8. Expansions (*m*/*z* 600–3000) of the ESI–MS/MS spectra from the 28-mer of PBMA A ([**2** + 2Cat]$^{2+}$), where Cat is lithium, sodium, potassium, rubidium or caesium.

where *m*/*z*(**G**$_{\mathbf{B}n}$) is the mass-to-charge ratio of a peak from the **G** series and *M*(*n***B**) and *M*(Cat) are as described above for Eqs. (8) and (9).

An expansion of the higher *m*/*z* region (*m*/*z* 600–3000) of the spectra from [**2** + 2Cat]$^{2+}$ precursors of PBMA A is displayed in Fig. 8. Although the ion peaks are significantly less intense than those of the **A** and **B** series observed below *m*/*z* 600, several series at relatively high signal-to-noise ratios are found in this higher *m*/*z* region of the spectra from lithiated, sodiated and potassiated precursors. Peaks are also present, at significantly lower signal-to-noise ratios in the spectrum from the [**2** + 2Rb]$^{2+}$ precursor ion, with no peaks detected in this region from the caesiated precursor. The peaks in these series are again separated by *m*/*z* 142, equivalent to the repeat unit mass of the PBMA polymer, indicating that singly charged fragment ions dominate in this region of the spectra as for the lower *m*/*z* expansions displayed in Fig. 7. It is noted that these singly charged fragment ion

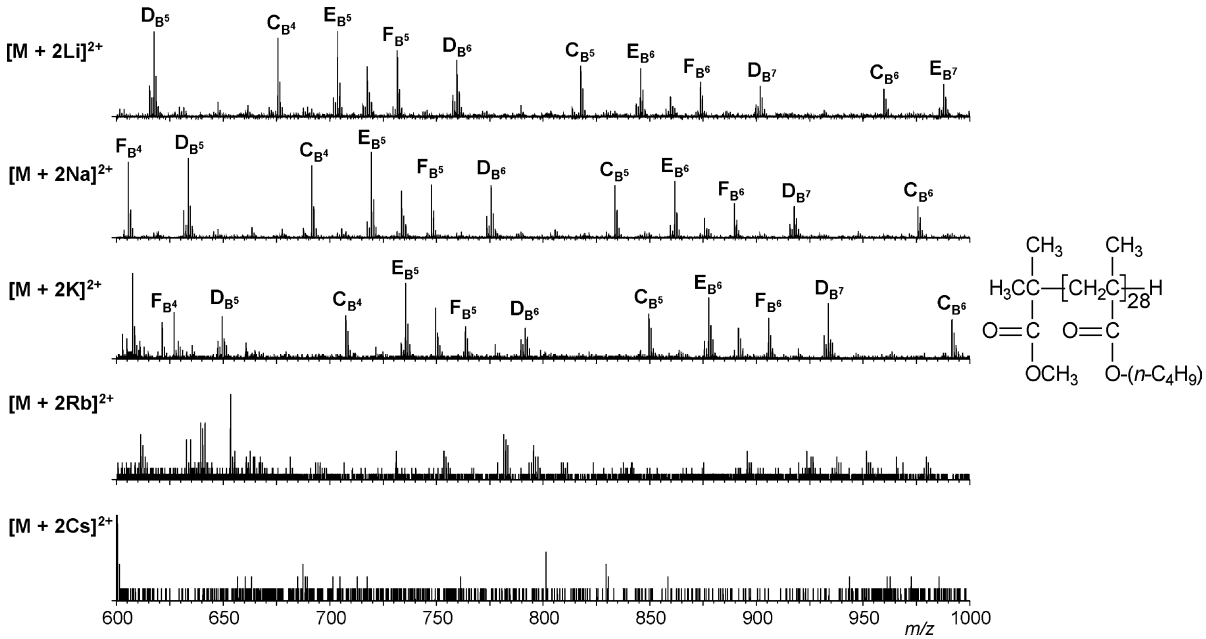

Fig. 9. Annotated expansions (*m*/*z* 600–1000) of the ESI–MS/MS spectra from the 28-mer of PBMA A ([**2** + 2Cat]$^{2+}$), where Cat is lithium, sodium, potassium, rubidium or caesium (see text for explanation of peak annotation).

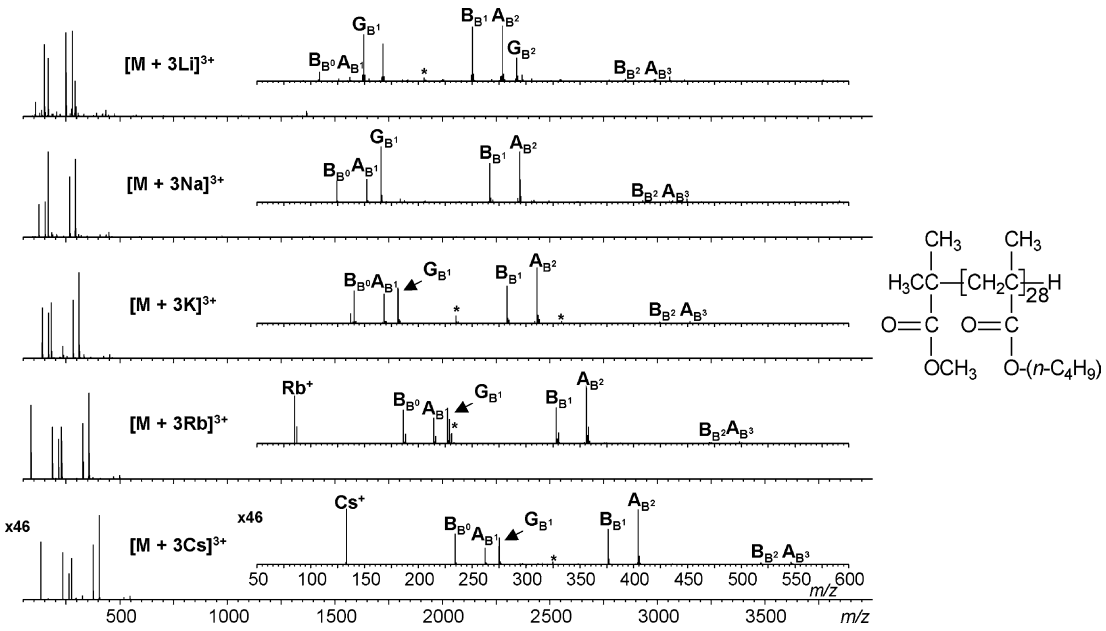

Fig. 10. ESI–MS/MS spectra (E_{coll} = 75 eV) from the 28-mer of PBMA A ([**2** + 3Cat]$^{3+}$), where Cat is lithium, sodium, potassium, rubidium or caesium (* peaks from alkali metal (Cat) acetate (Ac) clusters of the type [Cat_xAc_{x-1}]$^+$). Annotated expansions of the *m*/*z* 50–600 region are also shown (see text for explanation of peak annotation).

peaks extend to much greater mass-to-charge ratios in the fragment ion spectrum from the [**2** + 2K]$^{2+}$ precursor ion, when compared with the data from the lithiated and sodiated precursors.

A further expansion of this region of the spectra (*m*/*z* 600–1000) is displayed in Fig. 9. These data are annotated with the proposed assignments for the fragment ions. Five major series of singly charged fragment ions peaks may be seen, which are propounded to be analogous to the **C**, **D**, **E**, **F** and **G** series seen in the spectra from PMMA A and observed in MALDI-CID data from PBMA A [24]. The annotation is similar to that described above for the **A** and **B** series of PBMA A. The slight changes in this annotation from that described previously from MALDI-CID data [24] has been made to enable easier use for sequencing of copolymers by means of MS/MS, as described above. The pattern of peaks

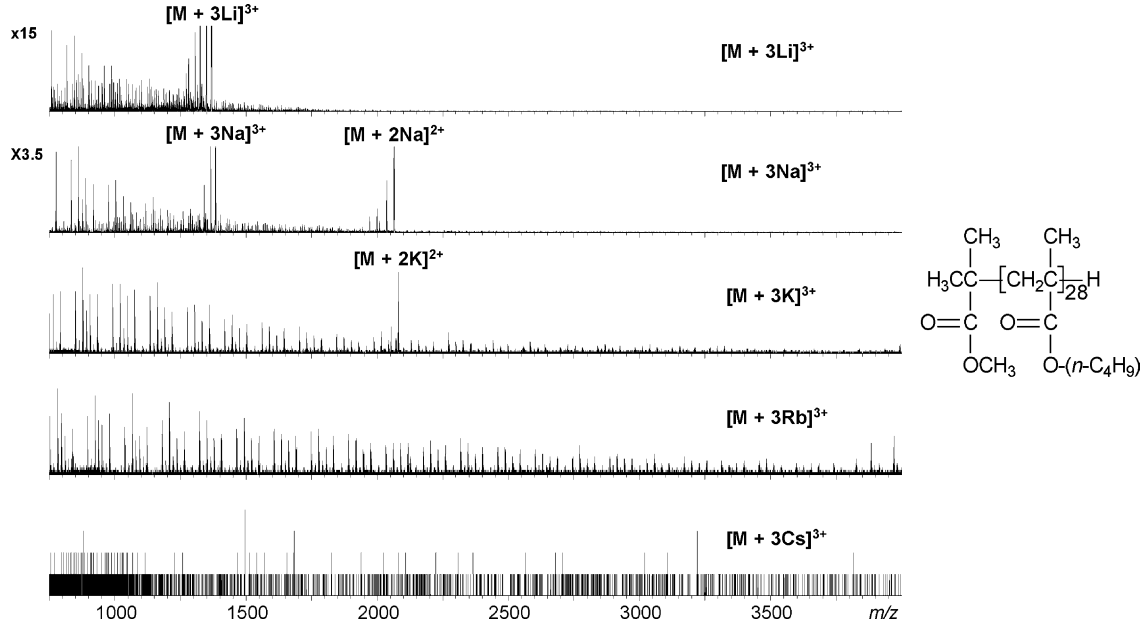

Fig. 11. Expansions (*m*/*z* 750–4000) of the ESI–MS/MS spectra from the 28-mer of PBMA A ([**2** + 3Cat]$^{3+}$), where Cat is lithium, sodium, potassium, rubidium or caesium.

from the **G** series, with a dominant peak at low *m/z* and peaks of decreasing intensity at higher mass-to-charge ratios (see Figs. 7 and 9), is the same as that observed previously from MALDI-CID data [24].

The mass-to-charge ratios of the singly charged fragment ion peaks from the **C**, **D**, **E** and **F** series, for PBMA, may be calculated from the following equations [24]:

$$m/z(\mathbf{C}_{\mathbf{B}n}) = M(\alpha) + M(n\mathbf{B}) - M(\mathrm{H}) + M(\mathrm{Cat}), \quad \mathbf{C}\ \text{Series} \tag{11}$$

$$m/z(\mathbf{D}_{\mathbf{B}n}) = M(\omega) + M(n\mathbf{B}) - M(\mathrm{C_5H_9O_2}) + M(\mathrm{Cat}), \quad \mathbf{D}\ \text{Series} \tag{12}$$

$$m/z(\mathbf{E}_{\mathbf{B}n}) = M(\omega) + M(n\mathbf{B}) - M(\mathrm{CH_3}) + M(\mathrm{Cat}), \quad \mathbf{E}\ \text{Series} \tag{13}$$

$$m/z(\mathbf{F}_{\mathbf{B}n}) = M(\alpha) + M(n\mathbf{B}) - M(\mathrm{C_4H_7O_2}) + M(\mathrm{Cat}), \quad \mathbf{F}\ \text{Series} \tag{14}$$

where $m/z(\mathbf{C}_{\mathbf{B}n})$, $m/z(\mathbf{D}_{\mathbf{B}n})$, $m/z(\mathbf{E}_{\mathbf{B}n})$ and $m/z(\mathbf{F}_{\mathbf{B}n})$ are the mass-to-charge ratios of a peak from the **C**, **D**, **E** and **F** series, respectively, and $M(\alpha)$, $M(\omega)$, $M(n\mathbf{B})$ and $M(\mathrm{Cat})$ are as described above for Eqs. (8) and (9). The structures for these fragment ions were proposed previously, from MALDI-CID data [24] and are analogous to those shown above for the same series from ESI–MS/MS of PMMA A.

The ESI–MS/MS spectra from the triply charged precursors of the 28-mer of PBMA A ($[\mathbf{2} + 3\mathrm{Cat}]^{3+}$) are shown in Fig. 10. Annotated expansions of the low *m/z* regions (*m/z* 50–600) of these product ion spectra are again also displayed. Singly charged fragment ion peaks in this area of the spectra are again dominant, as for the spectra from doubly charged precursors. The intensities of the fragment ion peaks follow a very similar pattern for both the spectra from the doubly and triply charged precursor ions from PBMA A (see expansions in both Figs. 7 and 10). The bare cation peak intensities (i.e. for Rb^+ and Cs^+) are similar in spectra from both the $[\mathbf{2} + 3\mathrm{Rb}]^{3+}$ and $[\mathbf{2} + 3\mathrm{Cs}]^{3+}$ precursor ions. The **A**, **B** and **G** series of peaks are all seen at similar intensities in both sets of spectra. These former two series of peaks can be employed to calculate the masses of the end groups, as described above (see Eqs. (8) and (9)).

An expansion of the higher *m/z* region (*m/z* 750–4000) of these spectra is displayed in Fig. 11. Residual precursor ion peaks can be seen in the spectra from lithiated and sodiated precursors ($[\mathbf{2} + 3\mathrm{Li}]^{3+}$ and $[\mathbf{2} + 3\mathrm{Na}]^{3+}$, respectively) and peaks from losses of one cation from the precursor are observed in the spectra from sodiated and potassiated precursor ions (i.e. $[\mathbf{2} + 2\mathrm{Na}]^{2+}$ and $[\mathbf{2} + 2\mathrm{K}]^{2+}$, respectively). The fragment ion spectra from the lithiated and sodiated precursor also appear very complex in the region below *m/z* 2000, which is a consequence of the presence of singly and doubly charged fragment ions. The doubly charged fragment ion peaks are more intense in the spectrum from $[\mathbf{2} + 3\mathrm{Li}]^{3+}$. Furthermore, triply charged fragment ion peaks are also observed, at a significantly lower intensity level, in the spec-

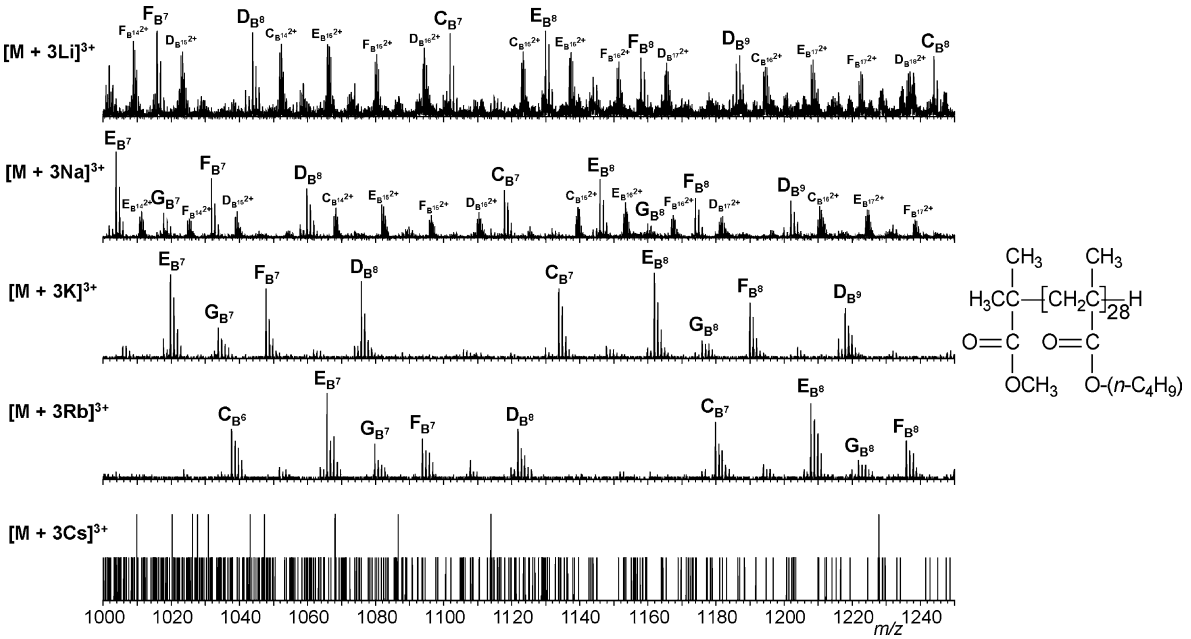

Fig. 12. Annotated expansions (*m/z* 1000–1250) of the ESI–MS/MS spectra from the 28-mer of PBMA A ($[\mathbf{2} + 3\mathrm{Cat}]^{3+}$), where Cat is lithium, sodium, potassium, rubidium or caesium (see text for explanation of peak annotation).

trum from the lithiated precursor ion. The greater intensity of multiply charged fragment ion peaks in spectra from the $[\mathbf{2} + 3\mathrm{Li}]^{3+}$ and $[\mathbf{2} + 3\mathrm{Na}]^{3+}$ precursors is a significant disparity between these data and that from the respective doubly charged precursor ions, where singly charged fragment ions are exclusive at noteworthy intensity values.

A further expansion of this region of the spectra (*m*/*z* 1000–1250) is displayed in Fig. 12, which are annotated as for previous data except that doubly charged fragment ion peaks are also noted (by a superscript 2+, e.g. $\mathbf{C_{B15}}^{2+}$ is a doubly charged fragment ion of the **C** series that contains fifteen whole or partial units of BMA). The mass-to-charge ratios of these doubly charged fragment ions of the **C**, **D**, **E** and **F** series may be calculated from the equations above (Eqs. (11)–(14)) by adding the mass of another cation to the values before dividing the sum by 2.

Singly charged fragment ion peaks are slightly more intense than those from the doubly charged species in this region of the spectra from lithiated and sodiated precursors, with singly charged fragments moieties being dominant from the $[\mathbf{2} + 3\mathrm{K}]^{3+}$ and $[\mathbf{2} + 3\mathrm{Rb}]^{3+}$ precursors. The added complexity in the higher *m*/*z* region of the spectra from lithiated and sodiated triply charged precursors, as a consequence of the significant intensity of doubly charged fragment peaks, makes interpretation of the data more time consuming for the PBMA homopolymer. It is therefore recommended that the potassiated and/or rubidiated precursors are selected for MS/MS experiments when higher molecular weight alkyl methacrylate homopolymers and, especially, copolymers are characterised (presuming the results will be analogous for other methacrylate polymers of this molecular weight). The use of these higher ionic radii cations would possibly be more appropriate when sequencing methacrylate copolymers of a similar molecular weight by means of MS/MS, as the ion peaks of the **C**, **D**, **E** and **F** series are employed for this purpose [24].

4. Conclusions

These data indicate that ESI–MS/MS may be used to characterise alkyl methacrylate homopolymers, such that information on end groups and backbone structure may be gleaned. The spectra, even from multiply charged precursor ions, are similar to that obtained previously from MALDI-CID experiments on singly charged precursors of the same polymers [20,24]. The high signal-to-noise ratios for ESI–MS/MS data from oligomers with molecular weights of greater than 4000 Da (see data from PBMA A) indicate that this technique may be employed to characterise significantly higher molecular weight alkyl methacrylate polymers. This will require selection of precursors with a higher charge state, as these species become prevalent for higher molecular weight polymers.

The option of direct connectivity of ESI with gel-permeation chromatography (GPC) has previously been demonstrated [36]. The high signal-to-noise ratios obtained in the ESI–MS/MS described here indicate that this technique may be employed on-line with GPC to offer further structural studies of complex polymer systems. This could include characterisation of mixtures of polymers and copolymers, which are often difficult to characterise by means of nuclear magnetic resonance (NMR) spectroscopy. The ions of the **C**, **D**, **E** and **F** series may be used to differentiate between alkyl methacrylate copolymers that are either block or random in nature.

References

[1] M.W.F. Nielen, Mass Spectrom. Rev. 18 (1999) 309.
[2] P.M. Peacock, C.N. McEwen, Anal. Chem. 76 (2004) 3417.
[3] S.D. Hanton, Chem. Rev. 101 (2001) 527.
[4] J.H. Scrivens, A.T. Jackson, Int. J. Mass Spectrom. 200 (2000) 261.
[5] C.N. McEwen, P.M. Peacock, Anal. Chem. 74 (2002) 2743.
[6] R. Murgasova, D.M. Hercules, Int. J. Mass Spectrom. 226 (2003) 151.
[7] C.M. Whitehouse, R.N. Dreyer, M. Yamashita, J.B. Fenn, Anal. Chem. 57 (1985) 675.
[8] J.B. Fenn, M. Mann, C.K. Meng, S.F. Wong, C.M. Whitehouse, Science 246 (1989) 64.
[9] M. Karas, D. Bachmann, U. Bahr, F. Hillenkamp, Int. J. Mass Spectrom. Ion Process. 78 (1987) 53.
[10] M. Karas, F. Hillenkamp, Anal. Chem. 60 (1988) 2299.
[11] D.C. Schriemer, L. Li, Anal. Chem. 68 (1996) 2721.
[12] A.G. Craig, P.J. Derrick, J. Am. Chem. Soc. 107 (1985) 6707.
[13] A.G. Craig, P.J. Derrick, J. Chem. Soc. Chem. Commun. (1985) 891.
[14] A.T. Jackson, K.R. Jennings, J.H. Scrivens, J. Am. Soc. Mass Spectrom. 8 (1997) 76.
[15] R.P. Lattimer, H. Munster, H. Budzikiewicz, Int. J. Mass Spectrom. Ion Process. 90 (1989) 119.
[16] R.P. Lattimer, Int. J. Mass Spectrom. Ion Process. 116 (1992) 23.
[17] R.P. Lattimer, J. Am. Soc. Mass Spectrom. 3 (1992) 225.
[18] R.P. Lattimer, J. Am. Soc. Mass Spectrom. 5 (1994) 1072.
[19] A.T. Jackson, H.T. Yates, J.H. Scrivens, G. Critchley, J. Brown, M.R. Green, R.H. Bateman, Rapid Commun. Mass Spectrom. 10 (1996) 1668.
[20] J.H. Scrivens, A.T. Jackson, H.T. Yates, M.R. Green, G. Critchley, J. Brown, R.H. Bateman, M.T. Bowers, J. Gidden, Int. J. Mass Spectrom. 165 (1997) 363.
[21] A.T. Jackson, A. Bunn, L.R. Hutchings, F.T. Kiff, R.W. Richards, J. Williams, M.R. Green, R.H. Bateman, Polymer 41 (2000) 7437.
[22] A.T. Jackson, R.C.K. Jennings, J.H. Scrivens, M.R. Green, R.H. Bateman, Rapid Commun. Mass Spectrom. 12 (1998) 1914.
[23] A.T. Jackson, J.H. Scrivens, W.J. Simonsick, M.R. Green, R.H. Bateman, Polym. Preprints 41 (2000) 641.
[24] A.T. Jackson, H.T. Yates, J.H. Scrivens, M.R. Green, R.H. Bateman, J. Am. Soc. Mass Spectrom. 8 (1997) 1206.
[25] A.T. Jackson, H.T. Yates, J.H. Scrivens, M.R. Green, R.H. Bateman, J. Am. Soc. Mass Spectrom. 9 (1998) 269.
[26] C.D. Borman, A.T. Jackson, A. Bunn, A.L. Cutter, D.J. Irvine, Polymer 41 (2000) 6015.
[27] A.R. Bottrill, A.E. Giannakopulos, C. Waterson, D.M. Haddleton, K.S. Lee, P.J. Derrick, Anal. Chem. 71 (1999) 3637.
[28] T. Yalcin, W. Gabryelski, L. Li, Anal. Chem. 72 (2000) 3847.
[29] A.T. Jackson, J.H. Scrivens, J.P. Williams, E. Shammel Baker, J. Gidden, M.T. Bowers, Int. J. Mass Spectrom.238 (2004) 287.
[30] R. Chen, L. Li, J. Am. Soc. Mass Spectrom. 12 (2001) 832.

[31] R. Chen, X.L. Yu, L. Li, J. Am. Soc. Mass Spectrom. 13 (2002) 888.
[32] M.A. Arnould, C. Wesdemiotis, R.J. Geiger, M.E. Park, R.W. Buehner, D. Vanderorst, Prog. Org. Coat. 45 (2002) 305.
[33] B.A. Cerda, D.M. Horn, K. Breuker, F.W. McLafferty, J. Am. Chem. Soc. 124 (2002) 9287.
[34] O. Laine, S. Trimpin, H.J. Rader, K. Mullen, Eur. J. Mass Spectrom. 9 (2003) 195.
[35] J. Gidden, A.T. Jackson, J.H. Scrivens, M.T. Bowers, Int. J. Mass Spectrom. 188 (1999) 121.
[36] L. Prokai, W.J. Simonsick, Rapid Commun. Mass Spectrom. 7 (1993) 853.